

Supporting Information

Selective Recognition of Fluoride Salts by Vasarenes: A Key Role of a Self-Assembled in situ Dimeric Entity Via an Exceptionally Short [O-H-O]⁻ H-Bond

R. Bengiat^a, M. Gil^a, A. Klein^a, B. Bogoslavsky^a, S. Cohen^a, F. Dubnikova^a,
G. Yardeni^b, I. Zilbermann^b and J. Almog^{*a}

^a Institute of Chemistry, The Hebrew University of Jerusalem, Jerusalem, 9190401, Israel.

^b Chemistry Department, Nuclear Research Centre Negev, Beer Sheva, 84190, Israel.

Supporting Information

Crystallographic Data and Structures, DFT data and UV-Vis, NMR, FT-IR Spectra:

Table S1. Crystallographic data and data collection parameters for **4-9**

Compound	4	5•EtOH	6•EtOH	7•EtOH	8•EtOH	9•2EtOH
Formula	C ₂₄ H ₁₄ O ₈	C ₂₆ H ₂₀ O ₉	C ₂₆ H ₂₀ Cs FO ₉	C ₂₆ H ₁₄ FO ₉ Rb	C ₃₄ H ₄₀ FNO ₉	C ₆₀ H ₅₈ FN ₂ O ₁₉
M	430.35	476.42	628.33	574.84	625.67	1130.08
T (K)	173(1) K	173(1)	173(1)	295(1)	173(1)	295(1)
λ (Å)	0.71073	0.71073	0.71073	0.71073	0.71073	0.71073
Crystal system	Triclinic	Monoclinic	Orthorhombic	Orthorhombic	Monoclinic	Triclinic
Space group	<i>P</i> $\bar{1}$	<i>P</i> 2 ₁ / <i>c</i>	<i>Pbca</i>	<i>Pbca</i>	<i>P</i> 2 ₁	<i>P</i> $\bar{1}$
a (Å)	7.5394(6)	10.811(1)	12.2617(9)	12.194(1)	9.5145(7)	9.749(1)
b (Å)	10.6149(9)	7.8640(8)	15.379(1)	15.536(2)	16.6525(1)	11.785(1)
c (Å)	12.161(1)	26.025(3)	25.646(2)	25.299(2)	9.5978(7)	14.738(2)
α (°)	84.000(1)					70.446(2)
β (°)	75.382(1)	99.560(2)			94.788(1)	86.671(2)
γ (°)	86.891(2)					71.563(2)
V (Å ³)	936.19(13)	2181.8(4)	4836.1(6)	4792.7(8)	1515.37(2)	1511.5(3)
Z	2	4	8	8	2	1
ρ _{calcd.} (Mg/m ³)	1.527	1.450	1.726	1.593	1.371	1.241
μ (mm ⁻¹)	0.116	0.111	1.594	2.129	0.103	0.095
Range of θ (°)	1.93–28.01	2.27–26.50	2.27–28.02	2.27–27.00	2.13–28.04	2.00–27.00
Total reflection	10887	22086	52953	49580	17714	16120
Independent reflection (R _{int})	4339	4507	5816	5225	7122	6446
Data with I > 2σ(I)	4339	4507	5816	5225	7122	6446
Parameters	304	321	355	369	416	412
R ₁	0.0606	0.0977	0.0254	0.0626	0.0527	0.0744
wR ₂ (I)	0.1277	0.1792	0.0635	0.1650	0.1275	0.2160

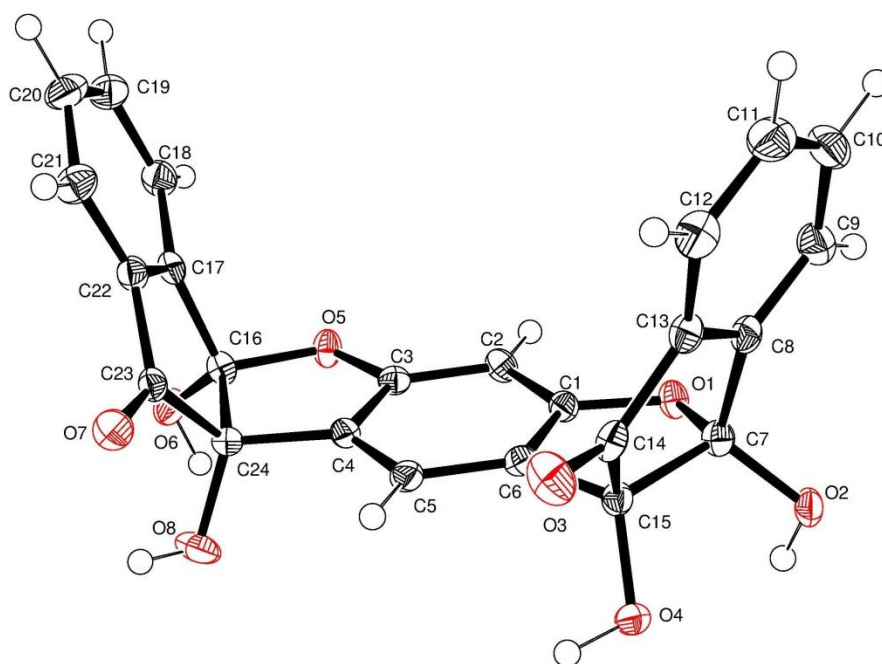


Figure S1. ORTEP drawing of vasarene-analogue **4**. The thermal ellipsoids are scaled to enclose 50% probability. Solvent molecules were hidden for clarity.

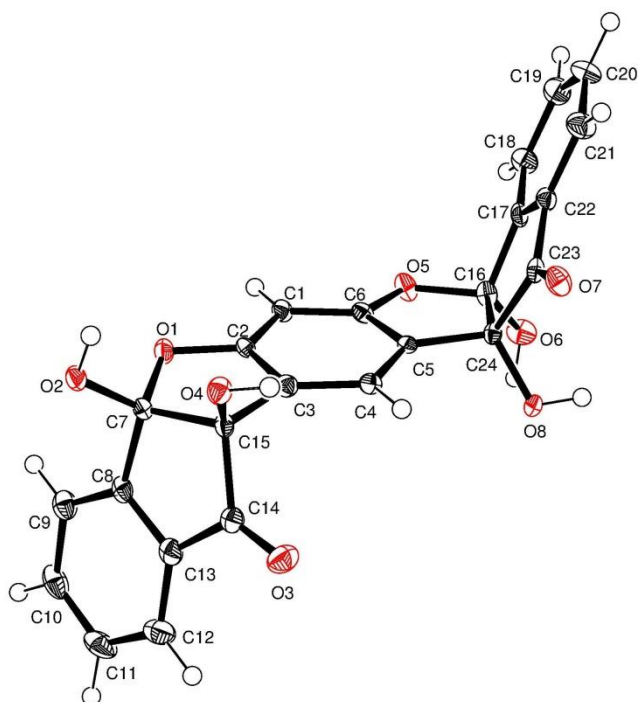


Figure S2. ORTEP drawing of vasarene-analogue **5**. The thermal ellipsoids are scaled to enclose 50% probability. Solvent molecules were hidden for clarity.

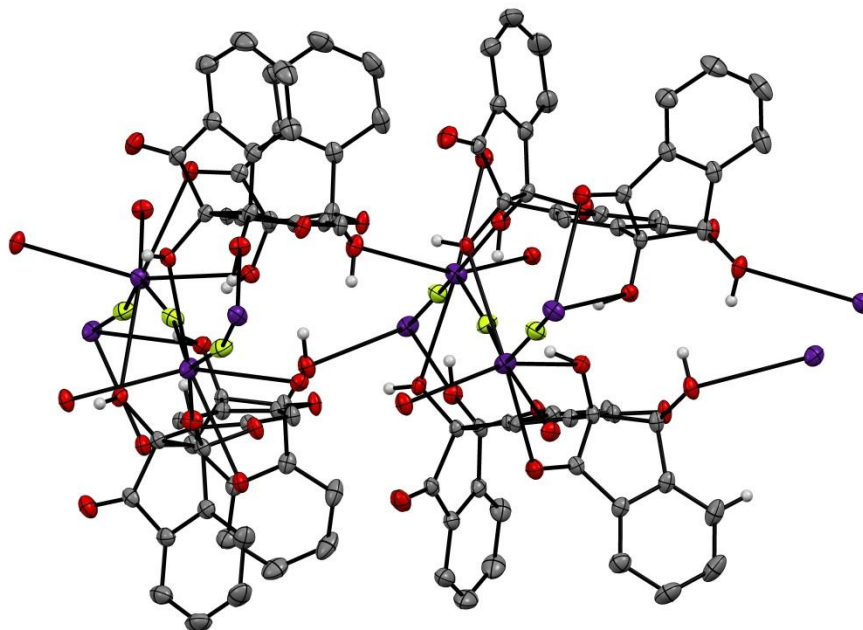


Figure S3. Mercury ORTEP-format drawing of CsF complex - **6** - 1x1x0.5 fragment of crystal packing. Purple - Cs⁺, lime - F⁻, red - oxygen. The thermal ellipsoids are scaled to enclose 50% probability. Solvent molecules and aromatic hydrogen atoms were hidden for clarity.

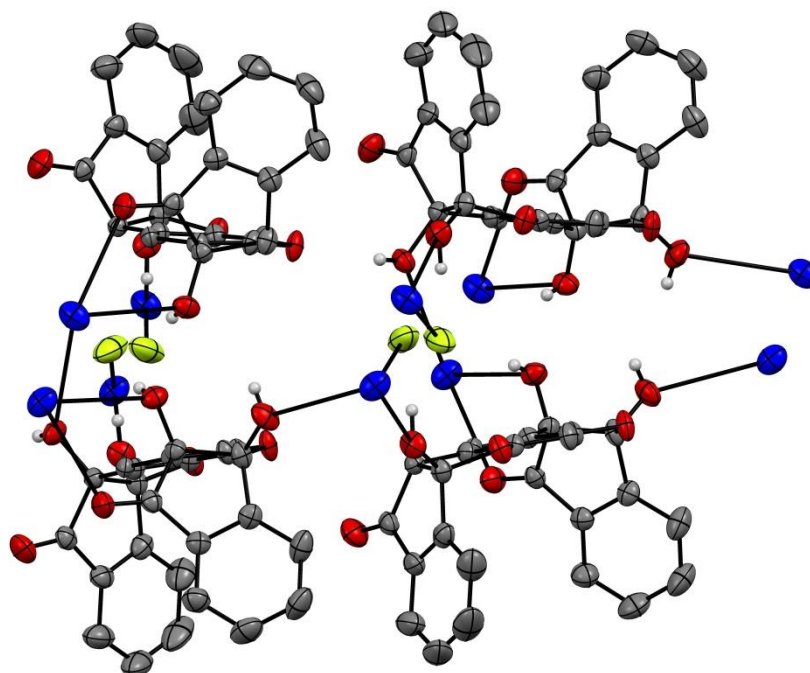


Figure S4. Mercury ORTEP-format drawing of RbF complex - **7** - 1x1x0.5 fragment of crystal packing. Blue - Rb⁺, lime - F⁻, red - oxygen. The thermal ellipsoids are scaled to enclose 50% probability. Solvent molecules and aromatic hydrogen atoms were hidden for clarity.

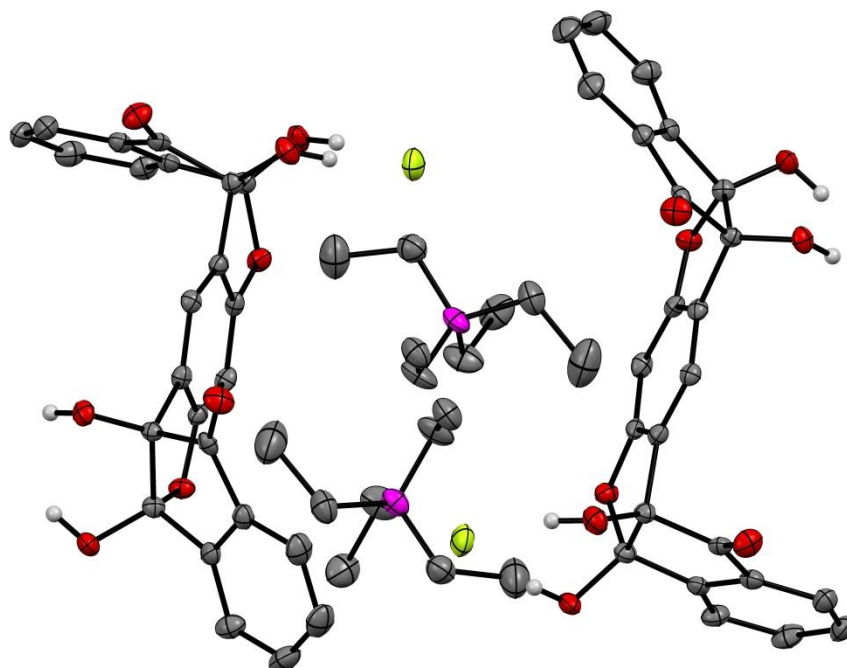


Figure S5. Mercury ORTEP-format drawing of tetraethyl ammonium fluoride complex - **8** – unit cell. Magenta – nitrogen, lime – F⁻, red – oxygen. The thermal ellipsoids are scaled to enclose 50% probability. Solvent molecules as well as aliphatic and aromatic hydrogen atoms were hidden for clarity.

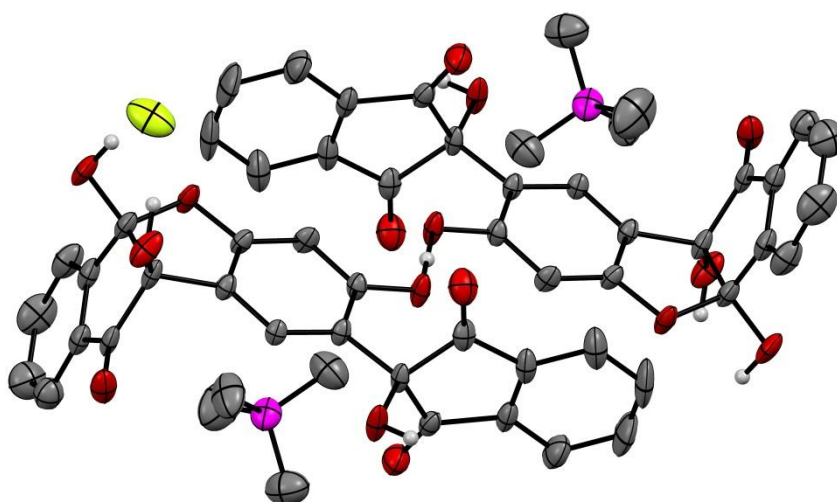


Figure S6. Mercury ORTEP-format drawing of tetramethyl ammonium fluoride complex - **9** –unit cell. Magenta – nitrogen , lime – F⁻, red – oxygen. The thermal ellipsoids are scaled to enclose 50% probability. Solvent molecules and aromatic hydrogen atoms were hidden for clarity.

Table S2. Calculated theoretical values of $\Delta E/\Delta G$ for the "boat" **4** and "chair" **5** isomers^[a]

Possible configuration	4 $\Delta E/\Delta G$	5 $\Delta E/\Delta G$
[b]	0.0/0.0	-0.1/-0.2
[c]	5.5/4.9	5.3/4.8
[d]	11.1/10.0	11.3/10.2

[a] The energy values are in kcal mol⁻¹ calculated for room temp'. The isomerization energy barrier is approx. 9 kcal mol⁻¹. For calculation techniques – see supplementary information. [b] All O-H groups turned toward O-atom of carbonyl group – most stable conformation. [c] Two O-H groups turned toward O-atom of carbonyl group, the other two in opposite direction. [d] All O-H groups turned in opposite direction of carbonyl groups' O-atoms.

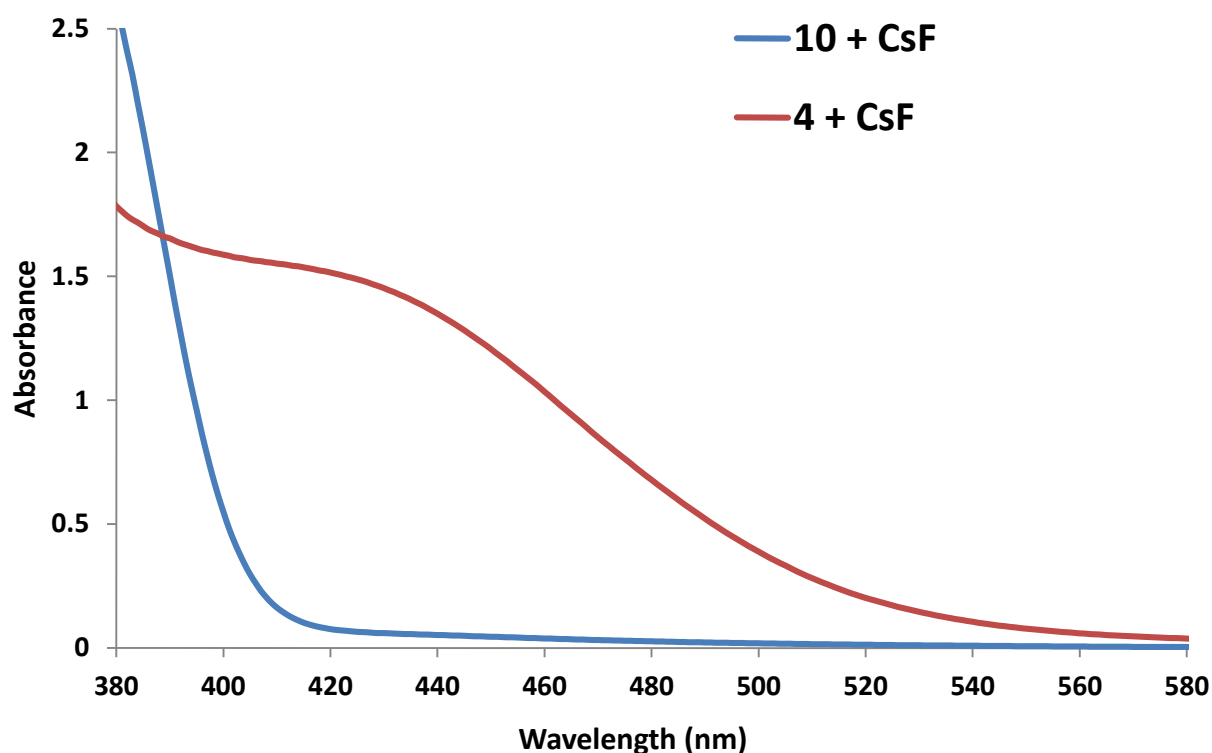
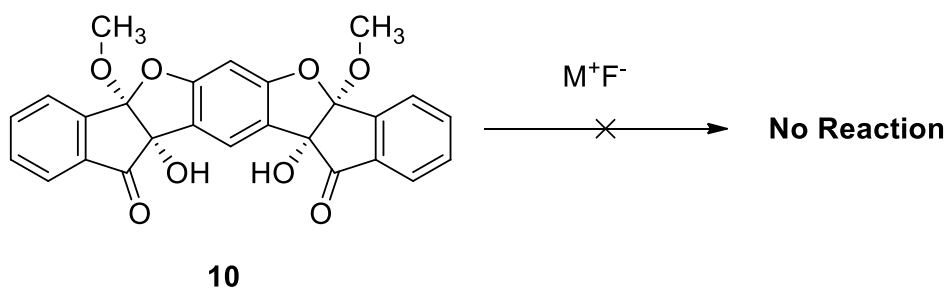


Figure S7. UV-vis absorption spectra of **4** and its protected derivative **10** with CsF in DMSO.



Scheme S1. Reaction of **10** with MF salts.

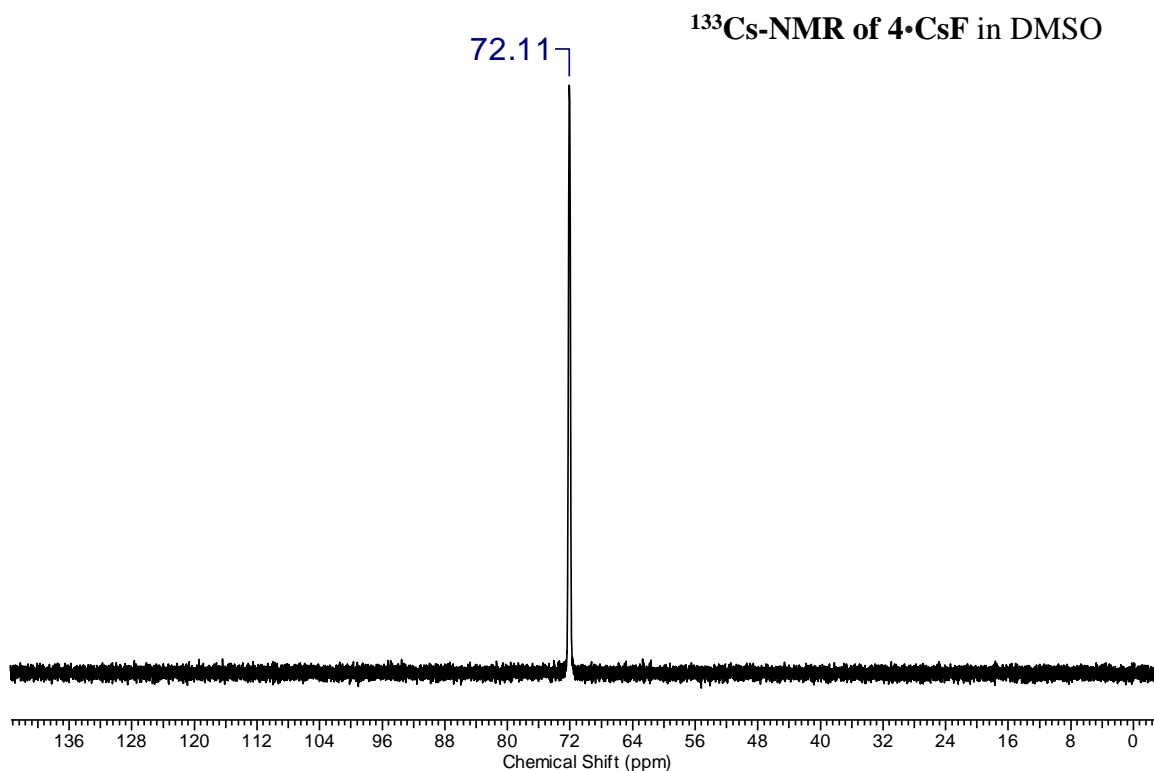


Figure S8. Complexation with vasarene-analogue **4** greatly enhances the solubility of the higher alkali fluorides in organic solvents such as DMF, DMSO. For **4**•CsF complex, the increased solubility is demonstrated by the appearance of a $^{133}\text{Cs-NMR}$ signal recorded on a 500 MHz Bruker Ultrashield Plus instrument. There is a clear shift in the signal from ~ 66.5 ppm of **1**•CsF complex^{S1} to 72.11 ppm of analogue **4**. As CsF is insoluble in DMSO there was no signal in $^{133}\text{Cs-NMR}$ ^{S1}.

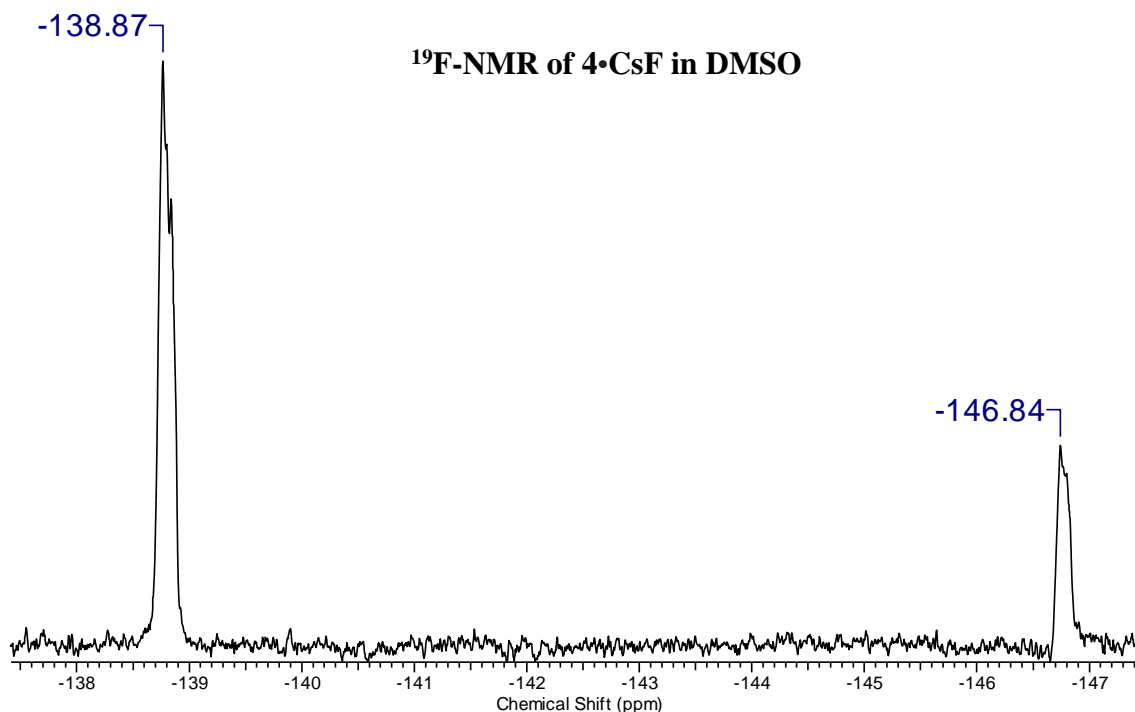


Figure S9. $^{19}\text{F-NMR}$ signals for **4**•CsF adduct in DMSO, recorded overnight on a 500 MHz Bruker Ultrashield Plus instrument. There are two signals, possibly assigned to slightly different fluorides in solution – at -138.87 ppm and -146.84 ppm. These chemical shifts were compared to reference CsF in D_2O with a signal at -122.2 ppm.

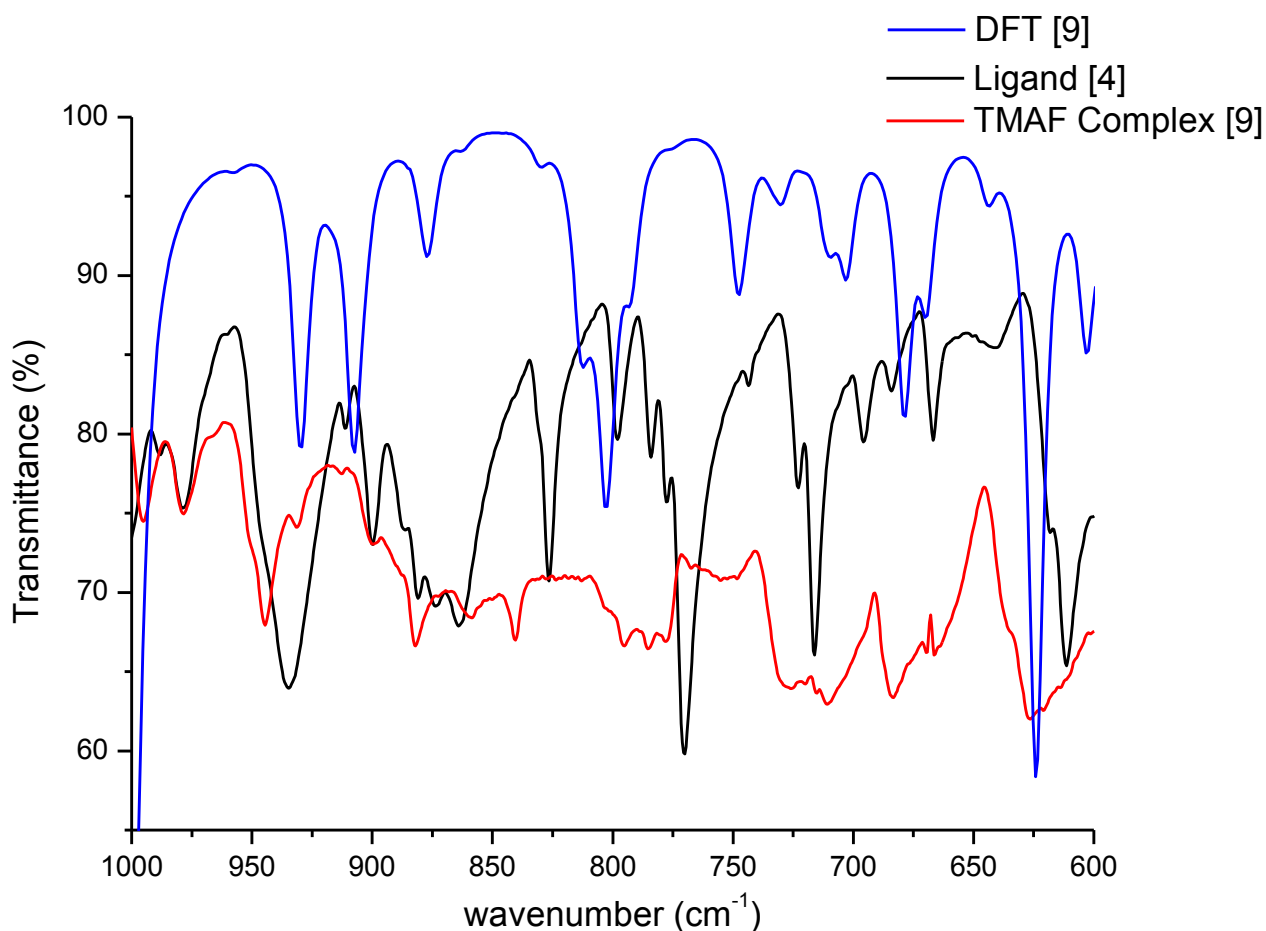


Figure S10. Solid state FT-IR spectra of complex **9** (red) compared to the ligand **4** (black). The strong broad band at 600-800 cm^{-1} is characteristic to proton vibrations of a short and symmetrical homo-conjugated [O-H-O]⁻ H-bond^{S2}. DFT calculations of theoretical IR vibrations for **9** (blue) coincide with the empirical bands (Table S3).

Table S3. FT-IR calculated DFT and empirical frequencies for [O-H-O]⁻ bond of complex **9**

DFT Frequency [cm^{-1}]	Empirical Frequency [cm^{-1}]	Description
624	621	O-H-O asymmetrical stretch
669	665	O-H-O asymmetrical stretch
679	680	O-H-O asymmetrical stretch
702	704	O-H-O bending
792	792	O-H-O bending

Materials and Instrumentation

All commercially available materials were purchased from Sigma-Aldrich, Alpha Aesar and Acros Organics. Deuterated solvents for NMR spectroscopy were obtained from Cambridge Isotope Laboratories.

The melting points were determined with an Electrothermal apparatus. ¹H NMR spectra were recorded with a 400 MHz Bruker DRX and a 500 MHz Bruker Ultrashield Plus instrument. ¹³³Cs and ¹⁹F-NMR spectra were recorded with a 500 MHz Bruker Ultrashield Plus instrument. FTIR spectra were recorded on a Bruker Tensor 27 FTIR-ATR spectrophotometer. Mass spectrometry was carried out by direct injection using an Agilent 6520 Accurate-Mass HR Q-TOF LC/MS apparatus (Agilent Technologies, United States). Absorbance measurements were carried out with a Varian Cary 100 Bio spectrophotometer by using a 4 mL cell.

X-ray Crystallography was performed as following: a single crystal of each compound was attached to a 400/50 MicroMeshes™ with NVH Oil^{S3}, and transferred to a Bruker SMART APEX CCD X-ray diffractometer equipped with a graphite-monochromator. Maintaining the crystal at -100°C was done with a Bruker KRYOFLEX nitrogen cryostat (for the relevant materials – **4-6, 8**). The system was controlled by a pentium-based PC running the SMART software package^{S4}. Data for **7** and **9** were collected at room temperature using MoK α radiation ($\lambda=0.71073$ Å). Immediately after collection, the raw data frames were transferred to a second PC computer for integration and reduction by the SAINT program package^{S5}. The structure was solved and refined by the SHELXTL software package^{S6}.

The IUPAC names of the products were generated using iChem Labs™ computer programme. The crystallographic structures were drawn using Mercury 3.6 (Build RC6) and ORTEP-3 2014.1 programmes.

The quantum chemical calculations were carried out using the density functional theory (DFT) method using Gaussian 09 code package. The calculations used the CAM-B3LYP^{S7} hybrid DFT functional. The Dunning correlation consistent polarized valence double ζ (cc-pVDZ) basis set was employed^{S8}. Structure optimization was performed by the Berny geometry optimization algorithm without symmetry constraints^{S9}. Vibrational analysis was performed in order to characterize the optimized structures as local minima. All the calculated frequencies, the zero point and the thermal energies correspond to harmonic oscillators.

References:

- S1 J. Almog, I. Gavish-Abramovich, R. Rozin, S. Cohen, G. Yardeni, I. Zilbermann, *Eur. J. Inorg. Chem.* 2012, **2012**, 4427–4432.
- S2 P. Barczyński, A. Komasa, M. Ratajczak-Sitarz, A. Katrusiak, B. Brzezinski, *J. Mol. Struct.*, 2006, **800**, 135–139.
- S3 MiTeGen, LLC P.O. Box 3867 Ithaca, NY 14852.
- S4 SMART-NT V5.6, BRUKER AXS GMBH, D-76181 Karlsruhe, Germany, 2002.
- S5 SAINT-NT V5.0, BRUKER AXS GMBH, D-76181 Karlsruhe, Germany, 2002.
- S6 SHELXTL-NT V6.1, BRUKER AXS GMBH, D-76181 Karlsruhe, Germany, 2002.
- S7 T. Yanai, D. P. Tew, N. C. Handy. *Chem Phys Lett.*, 2004, **393**, 51-57.
- S8 T. H. Dunning, Jr., *J. Chem. Phys.*, 1989, **90**, 107.
- S9 H. B. Schlegel, *J. Comput. Chem.*, 1982, **3**, 214.